JOURNAL OF TISSUE ENGINEERING AND REGENERATIVE MEDICINE
J Tissue Eng Regen Med (2009).
Published online in Wiley InterScience (www.interscience.wiley.com) **DOI:** 10.1002/term.229

RESEARCH ARTICLE

Axial vascularization of a large volume calcium phosphate ceramic bone substitute in the sheep AV loop model

Justus P. Beier[1]*, Raymund E. Horch[1], Andreas Hess[2], Andreas Arkudas[1], Johanna Heinrich[1], Johanna Loew[1], Heinz Gulle[3], Elias Polykandriotis[1], Oliver Bleiziffer[1] and Ulrich Kneser[1]
[1]*Department of Plastic and Hand Surgery, University Hospital of Erlangen, Germany*
[2]*Institute of Pharmacology and Toxicology, University of Erlangen, Germany*
[3]*Baxter Innovations GmbH, Vienna, Austria*

Abstract

Vascularization still remains an obstacle to engineering of bone tissue with clinically relevant dimensions. Our aim was to induce axial vascularization in a large volume of a clinically approved biphasic calcium phosphate ceramic by transferring the arteriovenous (AV) loop approach to a large animal model. HA/β-TCP granula were mixed with fibrin gel for a total volume of 16 cm^3, followed by incorporation into an isolation chamber together with an AV loop. The chambers were implanted into the groins of merino sheep and the development of vascularization was monitored by sequential non-invasive magnetic resonance imaging (MRI). The chambers were explanted after 6 and 12 weeks, the pedicle was perfused with contrast agent and specimens were subjected to micro-computed tomography (μ-CT) scan and histological analysis. Sequential MRI demonstrated a significantly increased perfusion in the HA/β-TCP matrices over time. Micro-CT scans and histology confirmed successful axial vascularization of HA/β-TCP constructs. This study demonstrates, for the first time, successful axial vascularization of a clinically approved bone substitute with a significant volume in a large animal model by means of a microsurgically created AV loop, thus paving the way for the first microsurgical transplantation of a tissue-engineered, axially vascularized bone with clinically relevant dimensions.

Received 25 June 2009; Revised 19 September 2009; Accepted 22 September 2009

Keywords tissue engineering; vascularization; angiogenesis; bone substitute; plastic surgery; microsurgery

1. Introduction

Reconstruction of extensive bone defects remains a major challenge in reconstructive surgery. While autologous bone grafting still remains the gold standard for osteogenic bone replacement, its inherent shortcomings and complications, such as limited availability of bone for harvest and significant donor-site morbidity, call for alternative approaches. A multitude of biomaterials have therefore been developed for bone tissue engineering, as well as ways to transplant cells into bony defects. However, most of these approaches are not feasible when extensive bone defects occur, where lack of vascularization often results in loss of transplanted cells or the non-integration of implanted biomaterial. To overcome these problems, tissue-engineered constructs have been generated which received their blood supply by axial vascularization through an arteriovenous pedicle. Among the various *in vivo* models of axial vascularization, the rat arteriovenous loop (AV loop) model seems most promising. It was introduced in by Erol and Spira (1979) in the context of flap prefabrication and then further developed for tissue-engineering purposes during the past decade (Bach *et al*., 2006; Arkudas *et al*., 2007, 2008). The axial type of blood supply

**Correspondence to: Justus P. Beier, Department of Plastic and Hand Surgery, University of Erlangen, Krankenhausstrasse 12, 91054 Erlangen, Germany.*
E-mail: Justus.beier@uk-erlangen.de

allows the vascularization and transfer of biomaterials independently of local conditions at the recipient site. We could previously demonstrate axial vascularization of other bone substitutes in a small animal AV loop model, with matrices displaying a significant degree of vascularization 8 weeks after implantation (Kneser *et al*., 2006). These promising results have led to the pivotal question – whether *de novo* creation of axially vascularized bone tissues in a human body is possible by employing the AV loop/isolation chamber model. This question has remained unanswered so far, since the AV loop has only been described in small animal experiments. After we recently established and characterized the sheep AV loop model as a new large animal model for axial vascularization (Beier *et al*., 2009), the present study investigates for the first time its application to vascularize a clinically approved bone substitute. To evaluate the course of vascularization of the implanted HA/β-TCP matrices over time, we used magnetic resonance imaging (MRI).

The combination of axial vascularization of a clinically approved HA/β-TCP matrix with clinically relevant dimensions and up-to-date imaging modalities may enable scaling-up the axial vascularization strategy from rats to sheep to clinical application.

2. Methods

2.1. Sheep AV loop model

German regulations for the care and use of laboratory animals were observed at all times. The animal care committee of the University of Erlangen and the government of Mittelfranken, Germany, approved all experiments. The animals were housed in the veterinary care facility at the University of Erlangen Medical Centre under standardized conditions of 55% air humidity and 20 °C room temperature, with a 12 h light/dark rhythm. The sheep were fed twice a day with 300 g standard sheep diet (Altromin GmbH & Co. KG, Lage, Germany) and hay and water *ad libitum*. The animals were deprived of food for 36 h prior to operation to limit regurgitation.

Anaesthesia and surgical procedure were performed as described previously (Beier *et al*., 2009). Briefly, sedation and analgesia of the sheep were induced by intramuscular (i.m.) administration of midazolam 0.2 mg/kg (Delta Select, Dreieich, Germany) and ketamine 10 mg/kg (Pfizer, Karlsruhe, Germany). A central venous line was inserted into the left jugular vein, since the operations were performed in the right lateral position. Subsequently, orotracheal intubation (7.5 Ch) was performed under laryngoscopic control. The respirator (Draeger, Luebeck, Germany) was adjusted to controlled artificial respiration intermittent positive pressure ventilation (IPPV) with a breath volume of 350 ml and breath frequency of 16/ min. Anaesthesia was maintained by inhalation of a gas mixture of 1–1.5% isoflurane (Baxter, Unterschleissheim, Germany) with air/oxygen. The passage of a stomach tube was performed into the paunch to prevent rumenal bloat. To adjust intra-operative fluid volume losses, the animals received an average 1000 ml Ringer–lactate during the operation. Peri-operatively, long-term amoxicillin (1 ml/10 kg) was administered i.m., followed by a post-operative application for 10 days (Vetoquinol Chassot GmbH, Ravensburg, Germany). Before opening of the anastomosis, 250 IU heparin were given intravenously (i.v.), followed by a post-operative daily subcutaneous (s.c.) dose of 2500 IU low-molecular-weight heparin. For post-operative analgesia, s.c. caprofen (0.4 mg/kg) was given. (Pfizer, Karlsruhe, Germany).

All operations were performed by the same microsurgeon, using a surgical microscope (Leica Microsystems, Wetzlar, Germany). On a total number of 12 female merino land sheep, each weighing 24–26 kg, the following operative procedure was performed.

The surgical site was shaved, prepped and draped for sterility. A longitudinal 12 cm skin incision reaching from the groin proximally down to the medial thigh aspect distally was performed. After dissection of the thin subcutaneous fatty layer, the translucent superficial fascia cruris was exposed and the vascular axis of the sapheneous artery, vein and nerve showed through. The superficial fascia was then divided over the vascular axis and the vessels were dissected microsurgically, starting from the origin in the groin, distally over a length of 12 cm. Side branches were coagulated using micro-bipolar forceps. After proximal clamping and distal ligation of artery and vein, micro-anastomosis was performed, using 9-0 Nylon interrupted sutures (Ethicon, Norderstedt, Germany). Following the creation of an AV loop between the proximal stumps of the left saphenous artery and vein, the AV loop was placed within the custom-made sterile isolation chamber. Chamber geometry and outer surface design were previously developed appropriate for implantation in the sheep's groin to enclose the AV loop (Beier *et al*., 2009). Arrises were avoided to decrease the risk of foreign body perforation through the sheep's skin. Four eccentric holes were drilled intro the base plate to allow fixation of the chamber to the underlying fascia by applying non-resorbable braided polyester sutures. Four rigid plastic pins were pierced outside-in through the base plate, reaching up to the inner surface of the lid in order to provide support for the AV loop within the chamber and to prevent the AV loop from retracting or slipping out of the chamber through the entrance gate. A cylindrical design for the inner moulding was chosen in order to achieve optimal similarity with the shape of the sheep's long bones; thus, later transplantation experiments into long bone defects may follow without change of the chamber design. A volume of 12 cm^3 HA/β-TCP granula (TRICOS) was first put inside the chamber. Voids between the granula were then filled with fibrin glue (composed as desribed below). After this the AV loop was placed around the four plastic pins onto the TRICOS–fibrin matrix. It was then embedded within a pure fibrin layer. On top of it a second layer of HA/ß-TCP granula was put into the chamber, its voids being filled with fibrin glue as within

DOI: 10.1002/term

the bottom layer (Figure 1). The clinically approved fibrin glue (Tisseel VH S/D Kit) was constituted by 2 ml fibrinogen (which had been diluted to a concentration of 20 mg/ml by adding fibrinogen buffer solution, as contained in the kit) together with 2 ml thrombin (500 IE/ml), using the Duploject Two Syringe System (all from Baxter Healthcare S. A., Wallisellen, Switzerland). The lid was closed and the chamber was fixed in the groin, using braided Polyester 1-0 sutures (Ethicon, Norderstedt, Germany). Haemostasis was assured, a closed suction drain was inserted, penetrating the sheep skin remote to the skin incision, and the wound was closed using Vicryl 3-0 (Ethicon).

2.2. Intra-vital MRI of AV-loop constructs

The volume of (neo)vascularization around the AV loop within the isolation chamber was evaluated by MRI at different time points (1, 3 and 6 weeks or 1, 6 and 12 weeks, respectively) after AV loop operation. Sedation for intravital imaging studies was performed as described previously (Beier *et al*., 2009). For prophylaxis and correction of fluid volume losses up to 1000 ml, crystalloid solution was given via the central venous line. MRI scans were measured on a Siemens Vision plus 1.5 T MRI Scanner (Siemens AG, Erlangen, Germany), using a neck flex coil wrapped around the leg in a fashion providing the best coverage of the implanted chamber; 5 ml gadofosveset trisodium contrast agent (Vasovist®, EPIX Pharmaceuticals Inc., Israel) was injected intravenously. This blood pool contrast agent causes a reduction in the T1 relaxation time, and consequently increased signal intensity, i.e. a positive image contrast. It is therefore not only suited for MR angiography but also selectively enhances the signal intensity in anatomical T1-weighted images. The diameters of the newly grown vessels around the AV loop are much below the resolution of our MR images. Nevertheless, we were able to identify voxels containing such small vessels due to the signal enhancement of the contrast agent within these vessels. Consequently, a T1-weighted three-dimensional (3D) dataset was scanned using a 3D FLASH (TR, 12 ms; TE, 5 ms; flip angle, 308, ACQ 2) covering a field of view of 200 × 200 × 118 mm, with a matrix size of 192 × 256 × 118 mm.

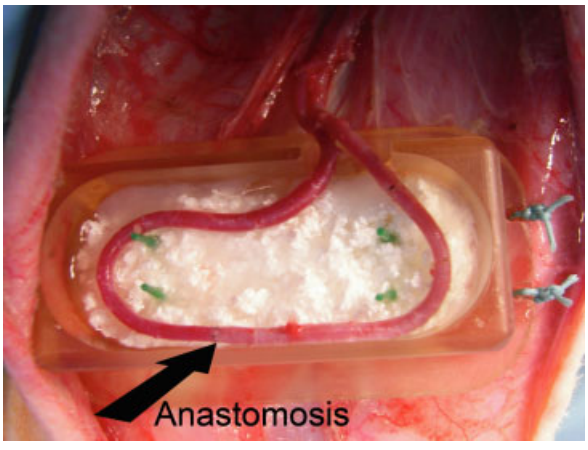

Figure 1. Intra-operative view of the sheep's groin: an isolation chamber containing the first half of the HA/β-TCP matrix infiltrated with fibrin glue. On the bottom half of this hybrid composite, a microsurgically created AV loop is placed and subsequently embedded in the upper half of the hybrid composite

2.3. Evaluation of the MR datasets

The data analysis was performed in the program MagnAn (© BioCom GbR), based on IDL (® ITT Visual Information Solution). The rationale was to segment all voxels above a certain threshold and use them as a correlate of increased vascularization caused by the increased intravasal contrast agent concentration of all vessels inside the voxel. At first, the isolation chamber, including the pedicle, was automatically segmented and used as a mask which was registered with the original dataset, sparing only voxels within the chamber. The segmentation threshold was determined based only on these voxels, as the mean grey value plus one-time standard deviation (SD). The threshold for a given animal was always determined at the first measurements and used for the following scans. The volume of (neo-)vascularized tissue was determined as the number of voxels above the given threshold. To generate an appropriate visualization of the original dataset, the segmentation mask and the segmented chamber inside were transferred to the program Amira® (Mercury Inc.). Here we displayed grey values of the inside of the chamber as a maximum intensity projection (MIP) onto the three surfaces. Within Amira, a surface of the voxel above threshold was generated, using a matching cube algorithm, measured and displayed as an isosurface (Figure 2a–c).

2.4. Statistics of the MR measurements

Since the absolute size of the implanted vessel was variable among the animals, we calculated fractional changes (DR/R) values for vessel volume and surface at weeks 3, 6 and 12 as compared to week 1 per animal, and plotted them over time. Significant differences between the different weeks were assessed by paired Student's *t*-tests. The *t*-tests were used for comparison between weeks 3, 6, 12 and 1, as well as from 6 and 12 to 3 and finally from 12 to 6.

2.5. Microfil® injection and micro-computed tomography (micro-CT)

Post-mortem imaging was performed as previously described (Beier *et al*., 2009). Briefly, the sheep were sacrificed 6 and 12 weeks after AV loop generation, by intravenous injection of a lethal dose of phenobarbital (Bayer, Leverkusen, Germany). Immediately before sacrifice, the animals received 5000 IU heparin intravenously.

DOI: 10.1002/term

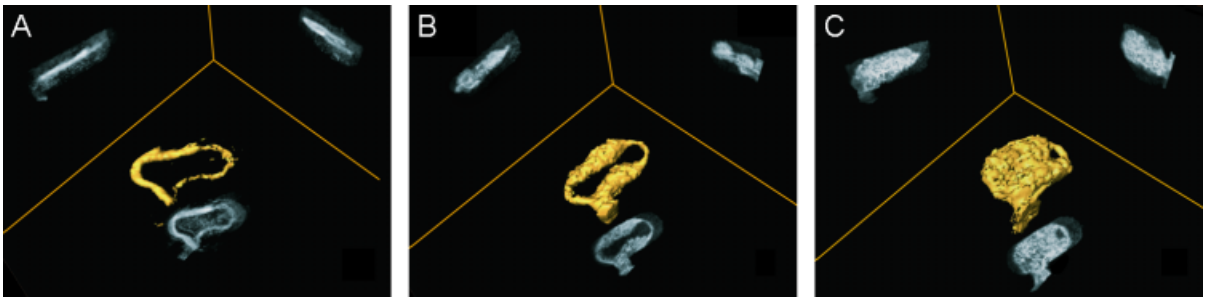

Figure 2. Serial MRI scans of one exemplary specimen, showing an increase in overall perfusion density and a development from one single dominant vessel towards an incremental collateralization. (A) 1 week; (B) 6 weeks; (C) 12 weeks

The isolation chambers were explanted *in toto*, the AV loop construct was removed from the chamber and the vascular pedicle was dissected under a surgical microscope. Artery and vein were identified and the arterial stump was perfused using 60 ml normal saline with heparin (5000 IU/ml). Subsequently, perfusion through the arterial stump was performed with 20 ml yellow Microfil® (MV-122) containing 5% MV Curing Agent (both from Flowtech, MA, USA). Finally, both vessel stumps were ligated and the constructs were cooled at 4 °C for 24 h and subsequently placed in 3.5% formalin. Following an 8 week period of decalcification in EDTA solution, micro-CT scans of the specimens were performed. The tube containing the explanted construct was placed on the table of a micro-CT scanner (Tomoscope 30s, VAMP GmbH, Erlangen, Germany). Scanning parameters were: tube voltage, 40 kV; voxel size, 40 µm; scan time, 3 min; radiation dose, 150 mGy.

2.6. Histological analysis of constructs

Histological analysis was performed as described previously (Kneser *et al.*, 2006). Briefly, specimens were fixed in formalin, decalcified in EDTA solution, dehydrated in graded ethanols and embedded in paraffin. Cross-sections (5 µm) were obtained from three standardized planes (one central, two peripheral), using a Leica microtome (Leica Microsystems, Wetzlar, Germany). Microphotographs were taken using a Leica microscope and Leica digital camera (Leica Microsystems). For histomorphometic analysis, three sections per specimen were examined. On each section, 24 defined standardized regions of interest (ROIs) were analysed. These regions were defined in a standardized fashion as arterial (A), venous (V), periphery of the artery (PA), periphery of the vein (PV) and centre of the construct (C) (Figure 4A). Images of these 24 ROIs were evaluated by two independent and blinded observers. All images were acquired with a Leica microscope and digital camera under × 100 magnification. The images were rendered bimodal (standardized threshold) with vessel lumina filled out in black (Figure 4B) (WinQ, Leica Microsystems, Bensheim, Germany). Vascular density was calculated for each group and each time. The results are given as mean ± standard deviation (SD). Statistical analysis was performed using two-tailed unpaired Student's *t*-test (after confirmation of Normal distribution by Kolmogorov–Smirnov test). The chosen critical level of statistical significance was $p < 0.05$.

3. Results

3.1. The sheep AV-loop model with HA/β-TCP implantation

Microvascular anastomoses of the saphenous artery and vein were successfully performed in all animals using an operation microscope and interrupted microsutures. Implantation of HA/β-TCP filled chambers with an embedded AV loop was facilitated in all 16 animals (Figure 1). The surgical procedure was tolerated well, without any complications in the majority of the animals. Sacrifice of the saphenous artery and vein did not cause any impairment of circulation to the distal part of the sheep's leg. Four animals had to be excluded before completion of the study due to peri- or postoperative complications which were not directly related to the AV loop creation, but to the surgical intervention itself (infection, pneumonia, e.g.). In two of the remaining 12 animals, occlusion of the AV loop was noted before the end of the study; these specimens were explanted and also excluded from the study.

3.2. Intra-vital imaging analysis of vascularization by MRI

MRI was tolerated well by all animals, including the administration of contrast agent (Vasovist®, EPIX Pharmaceuticals Inc., Israel). The patency of the AV loops in 10 of 12 sheep was assessed by MRI over time. In one sheep, occlusion of the AV loop was detected prior to signs of infection, which were only to be unveiled 48 h later. In the other excluded sheep, signs of infection occurred during the interval between two scans, so MR scanning did not interfere with the decision of exclusion. Furthermore, increased perfusion of the matrix within the chamber over time could be visualized by MRI (Figure 2A–C). By applying algorithms to calculate the fractional changes (DR/R) values for vessel volume and surface, a significant incremental vascularization was

DOI: 10.1002/term

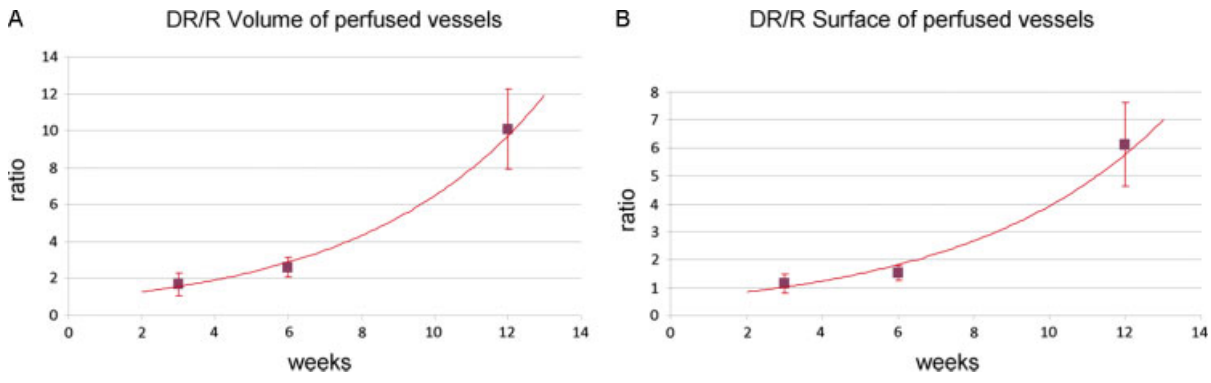

Figure 3. (A) Fractional changes (DR/R) values for vessel volume of weeks 3, 6, 12 to the week 1 (with value for week 1 = 1) per animal, showing statistical significance ($p < 0.05$, paired Student's *t*-test). (B) Fractional changes (DR/R) values for vessel surface of weeks 3, 6, 12 to the week 1 (with value for week 1 = 1) per animal, showing a statistically significant ($p < 0.05$, paired Student's *t*-test) increase in total surface of the perfused volume within the chamber as an indication for the outgrowing neo-vascular tree. Increase in total perfused volume within the chamber, indicating a constant vessel outgrowth, emerging from the main vascular AV-loop axis

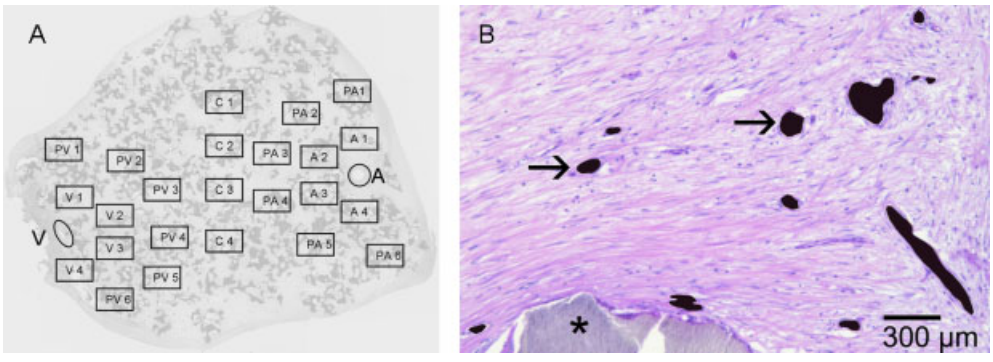

Figure 4. (A) Schematic drawing of a specimen after explantation demonstrating the approach to histomorphometric analysis with 24 defined standardized regions of interest (ROI). V, venous area; PV, periphery of the vein; A, arterial area; PA, periphery of the artery; C, central part of the specimen. (B) H&E staining of an explanted specimen, showing the black colour-coded (arrows) Microfil®-perfused vessels. *HA/β-TCP granula

observed over 3–12 weeks (Figure 3A, B). In some sheep, overall perfusion increased over time, while at the same time spatial distribution changed and heterogenicity of perfusion increased, with certain areas showing clearly enhanced perfusion compared to other areas.

3.3. Endpoint analysis: histology and micro-CT

Dense vascularization was detected in haematoxylin and eosin (H&E) staining of sections obtained from three representative sections of each explanted construct, which were orientated perpendicular to the AV loop axis. Perfused vessels could be clearly identified by the presence of black-appearing Microfil® solution inside the lumina, which could then be digitally marked with black colour (Figure 4B) before bimodal image rendering. Sprouting of newly forming capillaries was evident in the surroundings of the main vascular axis of the AV loop. Overall vascular density was lower 12 weeks after the AV loop operation compared to 6 weeks post-operatively, based on the total vessel count (Figure 5A), whereas there was a trend towards an increase in average vessel size (Figure 5B). There was an ingrowth of fibrous, vascularized tissue in between the HA/β-TCP granula reaching up to the centre of the construct. However, there were no histological signs of new bone formation.

Sprouting of vessels from the AV loop was visualized by micro-CT analysis of explanted AV loop HA/β-TCP constructs and subsequent 3D visualization. The results obtained by micro-CT could be positively correlated with histological analysis: there was a dense vascular network emerging from the AV loop. In contrast to the histomorphometrical data, the micro-CT data suggested an increase of vascular density from 6 to 12 weeks, while the tendency towards an increase of vessel size from 6 to 12 weeks could also be visualized by micro-CT (Figure 6A, B).

4. Discussion

In this study we present the sheep AV loop model as the very first large animal model for *de novo* creation of an axially vascularized bone substitute using microsurgical techniques. By adapting our recently established (Beier *et al.*, 2009) AV loop model in sheep, we

DOI: 10.1002/term

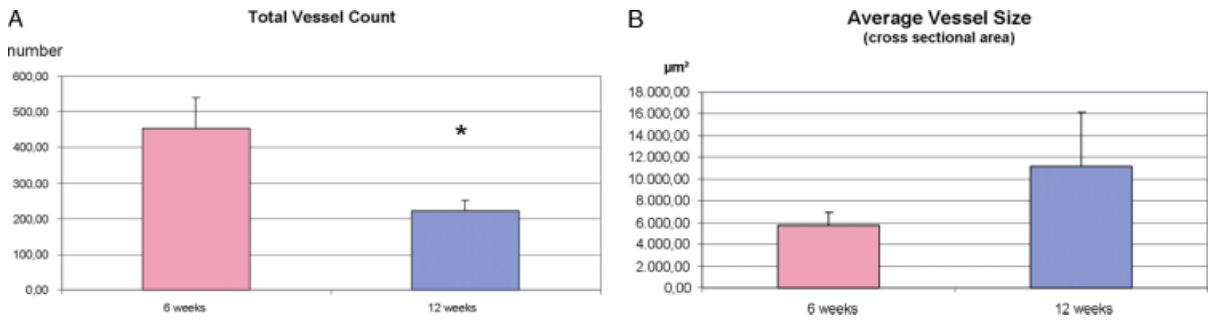

Figure 5. Bar diagrams showing the results of histomorphometric analysis. (A) A statistically significant decrease in vessel density was found after 12 weeks as compared to 6 weeks ($p < 0.05$). (B) A (statistically non-significant) tendency towards an increase of average vessel diameter was observed

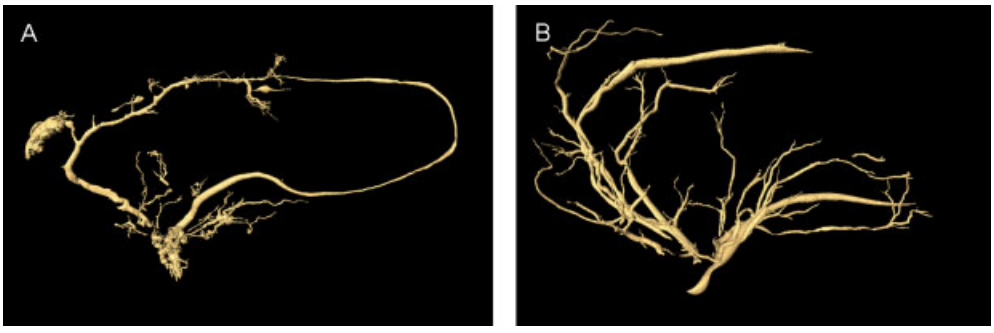

Figure 6. Micro-CT scans after explantation and Microfil® perfusion: (A) after 6 weeks, demonstrating sprouting of newly formed vessels; (B) after 12 weeks, showing development of large collateral vessels with loss of the smallest calibre (capillary) vessels at the periphery of the AV loop

were able to demonstrate *in vivo* formation of an axially vascularized completely isolated tissue construct with clinically relevant dimensions. Hence, transformation of the AV loop model from an animal model to clinical application may become a reality in the near future.

The ever-increasing demand for replacement options of lost tissues and organs is commonly met by either autologous transplantation of tissues from unharmed areas of the body, as performed by plastic surgeons on a daily basis, or allogenic transplantation of donor organs in the field of transplantation surgery. The tissue-engineering approach, as first propagated in the early 1990s, tries to overcome these obstacles (Langer and Vacanti, 1993). There had been countless studies, based on growing various autologous cell types on a myriad of different matrices, to generate tissue-engineering constructs *in vitro*. The major problem arises when *in vivo* application is intended, since the construct is not vascularized initially at the moment of implantation. Hence, most cells inside this construct will fail to survive the first days post-implantation. Nevertheless, the majority of currently applied tissue-engineering approaches rely on the so-called 'extrinsic' mode of neovascularization. In this setting, the neovascular bed originates from the periphery of the construct, which should be implanted into a site of high vascularization potential (Kneser *et al.*, 2006). Since oxygen and nutrition supply by diffusion is restricted to a maximum range of 200 µm into a given matrix (Goldstein *et al.*, 2001), suboptimal initial vascularization often limits the survival of cells in the centre of large constructs. Although generation of new tissue is feasible using these techniques, the newly formed tissue is vascularized in a random pattern, making a transfer to distant implantation sites impossible without destruction of the vascular network. Reconstructive surgeons therefore aim to generate so-called 'axially vascularized' tissues that could be transferred to the defect site using microsurgical techniques of vascular anastomosis. Since the initial description of the AV loop by Erol and Spira (1979), the superiority of the AV loop as a vascular carrier for an axial type of vascularization has been clearly demonstrated (Kneser *et al.*, 2006; Polykandriotis *et al.*, 2006, 2007). In a clinical scenario, the need for vascularized bone substitute emerges in cases with very large and/or complicated (e.g. irradiated or chronically infected), poorly vascularized bony defects. In these cases a tissue-engineered construct would not be implanted into the defect primarily, neither would it be possible to create it directly at the site of the defect, due to the impaired regenerative capacity and poor vascularization in the respective area. Instead, an arteriovenous loop would be created and placed into an isolation chamber together with the HA/β-TCP granula at a different, i.e. non-traumatized/non-irradiated region of the body. Upon axial vascularization (as shown in this study) and bone tissue formation (as the major aim for future studies, which could imply adding BMPs and/or osteogenic cells,

DOI: 10.1002/term

as well as mechanical force stimulation to induce bone formation), the whole *de novo*-formed bony construct could then be transplanted, in particular including microvascular anastomosis of the AV loop pedicle, into the site of the defect. In previous studies using a rat model, we were able to show that a combination of axial prevascularization of a fibrin matrix using an AV loop and secondary cell injection promotes the survival of injected myoblasts (Bach *et al*., 2006) and osteoblasts (Arkudas *et al*., 2007). The inner volume of 16 cm^3 in our chamber in a cylindrical shape emulates a given volume of tissue that certainly would not be sufficiently nourished by diffusion only, thus approaching clinically relevant dimensions. This is the first study demonstrating *de novo* formation of axially vascularized connective tissue overcoming the previous limitation to tissue volumes below 1 cm^3 (Bach *et al*., 2006; Lokmic *et al*., 2007; Morritt *et al*., 2007).

However, the way from engineering axially vascularized tissue to clinical application leads from small animal models such as rodents over large animal models such as ruminants, hence an isolated axial vascularization sheep model was recently introduced (Beier *et al*., 2009). In that large animal pre-study we used a pure fibrin matrix in the first animals as proof of principle. In the study presented here we now applied a clinically approved HA/β-TCP matrix as a further step towards engineering an axially vascularized bone substitute in a significant number of sheep to obtain representative results, while using a clinically relevant matrix. This biphasic ceramic is well established for clinical application, due to its osteoconductive properties. Unfortunately, the price for limiting the neovascularization to the axial vascular pedicle of the AV loop appears to be a too-challenging model for bone formation: while there is no bony contact at all, it might not be surprising that no evidence of new bone formation has so far been found histologically. Hence, it will be inevitable in the future to introduce osteoinductive, and possibly conductive, stimuli to finally achieve new bone formation. This may be facilitated through incorporation of autologous osteogenic cells such as bone marrow stromal cells, which could be implanted within the scaffold and have previously shown good osteogenic potential in other animal models (Cruz *et al*., 2008; Giannoni *et al*., 2008). The HA/β-TCP granula enable a dense vascularization but do not primarily display sufficient mechanical stability. However, the aim of this study was to induce and quantify axial vascularization of a clinically approved and established bone substitute matrix. During the next stage in vascularized bone tissue engineering, where the induction of bone tissue formation, including calcification of the densely vascularized construct, becomes relevant, bonding of the HA/β-TCP granula is expected. This will then provide mechanical stability over time, until sufficient stability for transplantation in a given bony defect is achieved. Hence, no mechanical testing of the granula matrix has been performed at this stage of the study, but will be of great interest at the time of inducing and assessing bone formation in our construct.

However, the AV loop model avoids the donor site morbidity of a whole latissimus dorsi muscle, which was taken into account for the first clinical attempt to create *de novo* axially vascularized, and thus transplantable, bone tissue (Warnke *et al*., 2004). Another important feature of this AV loop-based construct would be the degree of vascularization prior to transplanting it to the site of defect. Since in a clinical scenario end-point analysis such as histological examination or micro-CT are not applicable, new means of assessing vascularization inside such a construct must be established. In this study we could successfully demonstrate the ongoing process of increased perfusion of the HA/β-TCP construct within the chamber implantation. By using non-invasive MRI with a clinically approved, non-iodine contrast agent, the hazards that accompany CT scans, i.e. nephrotoxic contrast agents and X-ray exposure, were circumvented. We could successfully develop registration and segmentation algorithms for exclusive analysis of the vascularization inside the chamber. By appropriate image-processing algorithms and visualization techniques (e.g. maximum intensity projections) of the chamber contents, the significant perfusion increment over time could be demonstrated and the spatial distribution of neovascularized tissue was correlated with post mortem micro-CT findings and histology. In contrast to histomorphometric analysis as based on 2D sections, 3D perfusion quantification appears to be a valuable and more reliable tool for assessing the increased vascularization in such 3D tissue constructs. Especially when it comes to very small calibre vessels, deficient perfusion with viscous agents such as microfilm could have limitations, so that newly formed capillaries might be missed in histomorphometry and micro-CT scans. This could be an explanation for the decrease in vessels counted in histomorphometric analysis in this study, while MRI perfusion strongly suggests an incremental increase in vascular density over time. Even signs of an increasing collateralization were indicated by MRI, as well as an early detection of AV loop occlusion or the development of foreign body infection. In a clinical scenario, this method would be easily applicable in daily routine, wherever a common MRI scanner and the appropriate software are available. Therefore, the optimum point of time for transplanting the completely vascularized and perfused construct could be assessed non-invasively.

In summary, the sheep AV loop can be applied to induce an axial vascularization within a clinically approved bone substitute, with clinically relevant dimensions. Thus, the diffusion limit can be exceeded by far and the microvascular transplantation of such constructs may become feasible. With regard to clinical application, sequential MRI procedures, with subsequent registration and analysis of the perfused volumes, may elucidate the time course of vascularization patterns, as well as determination of the optimum transplantation time point. Further studies on how to induce bone formation inside the axially vascularized HA/β-TCP matrix will be necessary before reaching the next step towards clinical application.

DOI: 10.1002/term

Acknowledgments

The authors would like to thank S. Fleischer, K. Schubert, I. Arnold and Dr G. Pryymachuk (DVM) for their technical assistance, and L. Budinsky for excellent technical work on MRI. This work contains parts of J. Heinrich's and J. Loew's doctoral theses. The authors would like to thank Dr Edith Adamek (DVM) and Dr Dirk Labahn (DVM) for their competent help with anaesthesia of the sheep. The authors thank Professor P. Greil and P. Reinhard for production of the isolation chambers. This study was supported by the Baxter Healthcare Corporation and research grants from the University of Erlangen (ELAN Programme) and the Xue Hong and Hans Georg Geis foundation.

References

Arkudas A, Beier JP, Heidner K, *et al*. 2007; Axial prevascularization of porous matrices using an arteriovenous loop promotes survival and differentiation of transplanted autologous osteoblasts. *Tissue Eng* **13**: 1549–1560.

Arkudas A, Tjiawi J, Bleiziffer O, *et al*. 2007; Fibrin gel-immobilized VEGF and bFGF efficiently stimulate angiogenesis in the AV loop model. *Mol Med* **13**: 480–487.

Arkudas A, Tjiawi J, Saumweber A, *et al*. 2008; Evaluation of blood vessel ingrowth in fibrin gel subject to type and concentration of growth factors. *J Cell Mol Med* [28 Jun 2008, Epub ahead of print].

Bach AD, Arkudas A, Tjiawi J, *et al*. 2006; A new approach to tissue engineering of vascularized skeletal muscle. *J Cell Mol Med* **10**: 716–726.

Beier JP, Horch RE, Arkudas A, *et al*. 2009; *De novo* generation of axially vascularized tissue in a large animal model. *Microsurgery* **29**: 42–51.

Cruz DM, Ivirico JL, Gomes MM, *et al*. 2008; Chitosan microparticles as injectable scaffolds for tissue engineering. *J Tissue Eng Regen Med* **2**: 378–380.

Erol OO, Spira M. 1979; New capillary bed formation with a surgically constructed arteriovenous fistula. *Surg Forum* **30**: 530–531.

Giannoni P, Mastrogiacomo M, Alini M, *et al*. 2008; Regeneration of large bone defects in sheep using bone marrow stromal cells. *J Tissue Eng Regen Med* **2**: 253–262.

Goldstein AS, Juarez TM, Helmke CD, *et al*. 2001; Effect of convection on osteoblastic cell growth and function in biodegradable polymer foam scaffolds. *Biomaterials* **22**: 1279–1288.

Kneser U, Polykandriotis E, Ohnolz J, *et al*. 2006; Engineering of vascularized transplantable bone tissues: induction of axial vascularization in an osteoconductive matrix using an arteriovenous loop. *Tissue Eng* **12**: 1721–1731.

Langer R, Vacanti JP. 1993; Tissue engineering. *Science* **260**: 920–926.

Lokmic Z, Stillaert F, Morrison WA, *et al*. 2007; An arteriovenous loop in a protected space generates a permanent, highly vascular, tissue-engineered construct. *FASEB J* **21**: 511–522.

Morritt AN, Bortolotto SK, Dilley RJ, *et al*. 2007; Cardiac tissue engineering in an *in vivo* vascularized chamber. *Circulation* **115**: 353–360.

Polykandriotis E, Horch RE, Arkudas A, *et al*. 2006; Intrinsic versus extrinsic vascularization in tissue engineering. *Adv Exp Med Biol* **585**: 311–326.

Polykandriotis E, Tjiawi J, Euler S, *et al*. 2007; The venous graft as an effector of early angiogenesis in a fibrin matrix. *Microvasc Res* **75**: 25–33.

Warnke PH, Springer IN, Wiltfang J, *et al*. 2004; Growth and transplantation of a custom vascularised bone graft in a man. *Lancet* **364**: 766–770.

DOI: 10.1002/term